Journal of Cell Science 113, 4463-4474 (2000)
Printed in Great Britain © The Company of Biologists Limited 2000
JCS1845

Characterisation of transcriptionally active and inactive chromatin domains in neurons

Anna Akhmanova, Ton Verkerk, An Langeveld, Frank Grosveld and Niels Galjart*

MGC Department of Cell Biology and Genetics, Erasmus University, PO Box 1738, 3000 DR Rotterdam, The Netherlands
*Author for correspondence (e-mail: galjart@ch1.fgg.eur.nl)

Accepted 6 October; published on WWW 16 November 2000

SUMMARY

The tandemly organised ribosomal DNA (rDNA) repeats are transcribed by a dedicated RNA polymerase in a specialised nuclear compartment, the nucleolus. There appears to be an intimate link between the maintenance of nucleolar structure and the presence of heterochromatic chromatin domains. This is particularly evident in many large neurons, where a single nucleolus is present, which is separated from the remainder of the nucleus by a characteristic shell of heterochromatin. Using a combined fluorescence in situ hybridisation and immunocytochemistry approach, we have analysed the molecular composition of this highly organised neuronal chromatin, to investigate its functional significance. We find that clusters of inactive, methylated rDNA repeats are present inside large neuronal nucleoli, which are often attached to the shell of heterochromatic DNA. Surprisingly, the methylated DNA-binding protein MeCP2, which is abundantly present in the centromeric and perinucleolar heterochromatin, does not associate significantly with the methylated rDNA repeats, whereas histone H1 does overlap partially with these clusters. Histone H1 also defines other, centromere-associated chromatin subdomains, together with the mammalian Polycomb group factor Eed. These data indicate that neuronal, perinucleolar heterochromatin consists of several classes of inactive DNA, that are linked to a fraction of the inactive rDNA repeats. These distinct chromatin domains may serve to regulate RNA transcription and processing efficiently and to protect rDNA repeats against unwanted silencing and/or homologous recombination events.

Key words: Nucleolus, Chromatin, Methylation, Transcriptional repression, rRNA

INTRODUCTION

Eukaryotic interphase nuclei are highly compartmentalised structures. It is generally accepted that architectural organisation of the nucleus and regulation of transcription are functionally linked. For example, it has been proposed that RNAs are synthesised at ‘transcription factories’ – discrete sites within the nucleus, which contain high concentrations of a particular type of RNA polymerase and accessory factors (Cook, 1999). Different types of transcription factors are directed to nuclear subdomains by a variety of targeting signals (Stein et al., 1999). There is also significant evidence that transcriptional silencing is associated with targeting of genomic sequences to repressive (heterochromatic) nuclear compartments (Cockell and Gasser, 1999). The repetitive nature of a given DNA sequence could be a primary cause of its participation in heterochromatin, since repeated DNA is often repressed, or ‘silenced’, constitutively (Henikoff, 1998). Formation of heterochromatin is thought to protect the genome against unwanted recombination events at the repeated locus.

A vast number of regulatory factors, capable of activating or repressing transcription, have been characterised; however their organisation within the nucleus in relation to particular genomic sequences is largely unresolved. For example, it has been known for a long time that methylation of particular DNA sequences is often linked to their transcriptional inactivity. Recent studies have demonstrated that this phenomenon can be attributed, at least in part, to the action of specific methylated DNA-binding proteins, such as MeCP2, MBD1, MBD2 and MBD3 (Hendrich and Bird, 1998), some of which can form complexes with histone deacetylases and chromatin remodelling machinery (Bird and Wolffe, 1999). Such complexes are believed to alter chromatin structure and in this way contribute to regulation of transcription, however, their role in activation or repression of particular genomic loci remains to be determined.

The nucleolus is the most striking example of a correlation between specialised transcription and nuclear compartmentalisation, since in the nucleolus only the genes encoding ribosomal RNA (rRNA) are transcribed and its main function is that of ribosome biogenesis (Hadjiolov, 1985). Interestingly, in eukaryotes the rDNA genes are organised as tandem repeats. In the mouse diploid genome there are about 400 genes, which are spread over a number of different chromosomes, that vary according to the inbred strain analyzed (Kurihara et al., 1994). The murine rDNA repeat has a length of approximately 44 kb, of which 13 kb is transcribed into the 47S precursor rRNA (pre-rRNA) by a specialised

transcription complex, consisting of RNA polymerase I and accessory factors. This pre-rRNA is subsequently processed to 18S, 5.8S and 28S rRNAs, which are in turn assembled into ribosomes.

The number of rDNA copies, expressed in a given cell, depends on the demand for protein synthesis, and hence on metabolic activity. However, even in metabolically active cells not all rDNA copies are transcribed (Haaf et al., 1991) and therefore rDNA silencing must occur, in a cell and/or tissue specific manner. Since nucleolar structure appears to be regulated by proteins implicated in heterochromatin formation (Carmo-Fonseca et al., 2000) and rDNA genes have been found to undergo methylation (Bird et al., 1981), it is possible that some of the constitutively non-transcribed rDNA repeats are silenced because of DNA methylation (Brock and Bird, 1997). Thus, similar mechanisms may underly nuclear and nucleolar DNA repression. However, all the rDNA genes are very similar, which raises the question how inactive rDNA genes are distinguished from the active ones and how they are organised with respect to heterochromatin.

We are interested in the nuclear and nucleolar chromatin organisation of adult neurons and its correlation with gene expression, including that of rDNA (Mazarakis et al., 1996; Payen et al., 1998). This architecture is likely to reflect the requirements of efficient RNA synthesis, processing and transport without the superimposed complication of DNA replication and mitotic chromosome condensation, characteristic for dividing cells. Many neurons are metabolically active cells with large cytoplasmic volumes, the notable exception being granule cells of the cerebellum (Peters et al., 1991). The high protein synthesis requirements of large neurons presumably demand a similarly high ribosome biogenesis, which would account for the large size of the neuronal nucleolus. In addition, the majority of neuronal nucleoli contain a characteristic rim of nuclear heterochromatin, which can be stained with Hoechst and propidium iodide in tissue sections (Manuelidis, 1984a; Manuelidis and Borden, 1988) and the centromeric regions of many chromosomes are found clustered and attached as large aggregates to the neuronal nucleolus (Manuelidis, 1984b). The perinucleolar heterochromatic ring is surrounded by relatively 'open' chromatin, since this DNA is more accessible to DNAse I.

To investigate the functional significance of neuronal chromatin domains, we have developed modified RNA and/or DNA fluorescent in situ hybridisation (FISH) techniques, which are combined with immunofluorescent detection of chromatin proteins. These combined DNA and/or RNA FISH/immunofluorescence approaches allow simultaneous detection of nucleic acid sequences and antigens in paraffin-embedded brain tissue. We show here that in many adult neurons from inbred FVB mice, large arrays of inactive, methylated rDNA repeats tend to cluster near the centromere on the inside of the perinucleolar heterochromatin. Surprisingly, unlike other highly methylated genomic sequences, such as centromeric satellites, they do not contain a significant amount of MeCP2. Our data provide direct cytological evidence for non-random distribution of a methyl-CpG binding protein over methylated genomic DNA and indicate that silencing of a fraction of the rDNA genes is intimately associated with perinucleolar heterochromatin.

MATERIALS AND METHODS

Mice

Adult FVB mice were chosen for the majority of the experiments described in this report, since this inbred strain is used in our laboratory for standard breeding purposes and to generate transgenic lines. In the methylation experiment, shown in Fig. 4, DNA from FVB mice was compared to that of an age-matched C57Bl6 control mouse.

Molecular biology techniques

A murine cosmid library (Mazarakis et al., 1996) was screened with a ribosomal DNA probe (u5′ETS, positions 5611-5928 in the mouse rDNA gene sequence; accession number X82564; see Fig. 2A), that was labeled to high specific activity using a PCR protocol from the manufacturer (Boehringer). Of the 180 positive clones, 5 were investigated in more detail (cosmids labelled 3, 5, 7, 13 and 17 in Fig. 2A). For FISH a >11 kb *Sal*I fragment from cosmid 5 was used to detect non-transcribed rDNA (NTS probe), while the complete insert of cosmid 13 was used to detect transcribed rDNA (TS probe).

Genomic DNA was isolated and digested using standard procedures (Sambrook et al., 1989) and blotted onto Hybond N^+ membranes (Amersham). RNA was extracted from different mouse tissues (Auffray and Rougeon, 1980) and approximately 15 μg of total RNA was fractionated (Fourney et al., 1988) and blotted onto Hybond N^+ membranes. Probes were labeled using the random prime method (Feinberg and Vogelstein, 1983), or by PCR. Blots were exposed to PhophorImager screens (Molecular Dynamics).

Antibodies

The anti-MeCP2 antibodies (Nan et al., 1996) were a gift from Dr A. Bird (rabbit polyclonal #674, used as full serum in a 1:500 dilution); monoclonal anti-5-methylcytosine antibodies (Reynaud et al., 1992) were provided by Dr A. Niveleau (shipped as ascites fluid, used at 1:30 dilution); rabbit polyclonal anti-histone H1 antisera were gifts from Dr M. Bustin (affinity purified serum; dissolved at 0.2 mg/ml) and Dr M. Parseghian (Parseghian et al., 1993) (both antisera were used at 1:200 dilution); the rabbit polyclonal anti-coilin antiserum 204,10 (Santama et al., 1996) was a gift from Dr J. Sleeman (used at 1:200 dilution). Rabbit polyclonal anti-Eed antiserum (Denisenko and Bomsztyk, 1997) was a gift from Dr O. Denisenko (used at 1:200 dilution). Antisera against other Polycomb factors were tested, but did not work on brain paraffin sections. FITC-labeled goat anti-rabbit antibodies (Nordic Laboratories, The Netherlands; 1:80) and rhodamine-labeled sheep anti-mouse antibodies (Boehringer Mannheim; 1:25) were used for indirect immunofluorescence detection.

Immunocytochemistry and FISH

Paraffin-embedded tissue sectioning and antibody incubations were performed as described before (Payen et al., 1998), with a minor modification for MeCP2 detection: after microwave treatment the tissue sections in buffer were quickly chilled on ice because this gave a clearer signal. FISH was based on published protocols (Mulder et al., 1995; Wijgerde et al., 1995), with modifications.

For detecting RNA, rehydrated tissue sections were treated with 0.01% pepsin in 0.01 M HCl for 5 minutes at 37°C, rinsed in PBS, postfixed in 3.7% formaldehyde in PBS, rinsed several times in PBS and then in water, and dehydrated through an ethanol series and air dried. For detection of DNA, rehydrated tissue sections were fixed in 4% paraformaldehyde in PBS for 1 hour, rinsed several times in water and incubated for 1 hour with 100 μg/ml RNAse in water. Subsequently, slides were treated with 0.01% pepsin in 0.01 M HCl for 5 minutes at 37°C, rinsed in PBS, postfixed in 3.7% formaldehyde in PBS, rinsed several times in PBS and then in water. DNA was denatured by microwave treatment (10 minutes at 750 watts to bring the solution to the boiling-point and 2 minutes at 90 watts in 1 liter of 10 mM citrate buffer (pH 6.0)); the slides were immediately chilled

in ice-cold 70% ethanol, transferred to 96% ethanol and air-dried. For both RNA- and DNA-FISH, the hybridisation solution (50% formamide, 10% dextran sulfate, 2× SSC, 50 mM sodium phosphate buffer (pH 7.0), 1 mM EDTA, 200 ng/μl denatured salmon sperm DNA and 1-5 ng/μl probe), was applied to dry tissue sections, and the slides were incubated overnight in a moist chamber at 37°C. Slides were washed once in 2× SSC at room temperature, and then twice for 15 minutes in 0.2× SSC at 50°C. Subsequently, slides were rinsed in 25 mM Tris (pH 7.5), 100 mM NaCl, 0.05% Tween-20 (TNT buffer) and then blocked with 1% bovine serum albumin in TNT for 30 minutes at room temperature. Antibody incubations were performed in TNT buffer, each incubation for 1 hour at room temperature. After incubation with primary, secondary or tertiary antibodies, slides were rinsed 4 times 5 minutes in TNT buffer.

For FISH the following probes were used: u5′ETS, labeled with digoxigenin-11-dUTP (Boehringer) by PCR; NTS and TS rDNA probes, labeled with digoxigenin-11-dUTP or biotin –16-dUTP by nick-translation, mouse γ-satellite probe (an oligonucleotide with the sequence 5′-GGACCTGGAATATGGCGAGAAAACTGAAAAT-CACGGAAAATGAGAAATAC-3′, labeled with digoxigenin at position 25 and at the ends (Eurogentec, Belgium)). For detection of digoxigenin-labeled probes rhodamine- or FITC-labeled sheep anti-digoxigenin antibodies (Boehringer Mannheim; 1:50-1:100) were used, and for rDNA detection the signal was amplified using Texas Red or FITC-labeled donkey anti-sheep antibodies (Jackson Laboratories: 1:100). For detection of biotin-labeled probes, Texas Red-labeled avidin D (Vector Laboratories; 1:500) was used in the first detection step, followed by incubation with biotinylated goat anti-avidin antibodies (Vector Laboratories; 1:500) and then another incubation with Texas Red-labeled avidin D.

For simultaneous detection of rRNA transcripts and rDNA, tissue sections were hybridised first with digoxigenin labeled u5′ETS probe and, after incubation with FITC-labeled anti-digoxigenin antibodies, sections were fixed for 2 hours at room temperature in 4% paraformaldehyde in PBS, rinsed in water, microwave-treated for DNA denaturation, dehydrated and hybridised with a biotin-labeled NTS rDNA probe. Biotin detection was performed as described above. In the immuno-FISH protocol (with anti-histone H1 or anti-MeCP2 antibodies), the detection of proteins was performed together with that of the probe (the hybridisation step did not affect the reactivity of the above mentioned antibodies). For detection of 5-methylcytosine, tissue sections were pre-treated as for DNA-FISH, but after microwave treatment they were incubated in 2 M HCl for 1 hour at room temperature, neutralized in 0.1 M borate buffer (pH 9.0), rinsed with TNT, blocked and incubated with antibodies. Combined 5-methylcytosine – rDNA detection was performed in two different ways which yielded very similar results. The first method included tissue pre-treatment and incubation with anti-5-methylcytosine antibodies as described above. After incubation with secondary (FITC-labeled anti-mouse) antibodies, slides were fixed for 2 hours at room temperature in 4% paraformaldehyde in PBS, rinsed in water, microwave-treated for the second time, and hybridised with a biotin-labeled NTS rDNA probe, followed by biotin detection. Alternatively, slides were pre-treated as for 5-methylcytosine detection, but after 2 M HCl and 0.1 M borate treatment, slides were rinsed in water, dehydrated through an ethanol series and hybridised with a biotin-labeled NTS rDNA probe. After biotin detection slides were fixed with paraformaldehyde and microwave treated as in the first method, and incubated with anti-5-methylcytosine antiserum and the corresponding secondary antibodies.

The chromosomal localisation of rDNA loci in FVB mice was done using biotin labeled cosmid 7, and the following digoxigenin labeled telomere probes (Genome Systems Inc): for chromosome 12 probe 6852, for chromosome 15 probe 7734, for chromosome 18 probe 7771 and for chromosome 19 probe 6942 (Shi et al., 1997). Slides were mounted in DAPI/DABCO/Vectashield solution (Vector Laboratories).

Signals were captured with a Leica DMRBE fluorescence microscope, equipped with a Hamamatsu C4880 DCC, or with a Zeiss confocal laser scanning microscope (LSM510). In the latter case, optical sections of 0.7-0.9 μm were used.

RESULTS

Generation of probes for in situ detection of rRNA transcripts and rDNA repeats

In cultured cells, nucleolar transcription has been studied with the use of the first 600 bp fragment of the 5′ external transcribed spacer (5′ETS) of the rDNA repeat, because this fragment is rapidly cleaved from the 13 kb rRNA precursor and is postulated to be highly unstable (Gurney, 1985; Lazdins et al., 1997; Miller and Sollner-Webb, 1981). We therefore generated the unstable 5′ETS probe (u5′ETS, see Fig. 2A) and tested it on northern blot in mouse brain and kidney (Fig. 1). Surprisingly, while in kidney RNA only one major fragment of 13 kb could be detected, in brain the u5′ETS probe hybridises to 3 transcripts, of 13, 6.6 and 0.6 kb. The 13 kb RNA represents the full-length rRNA precursor. The 0.6 kb fragment, detected only in brain, presumably represents the

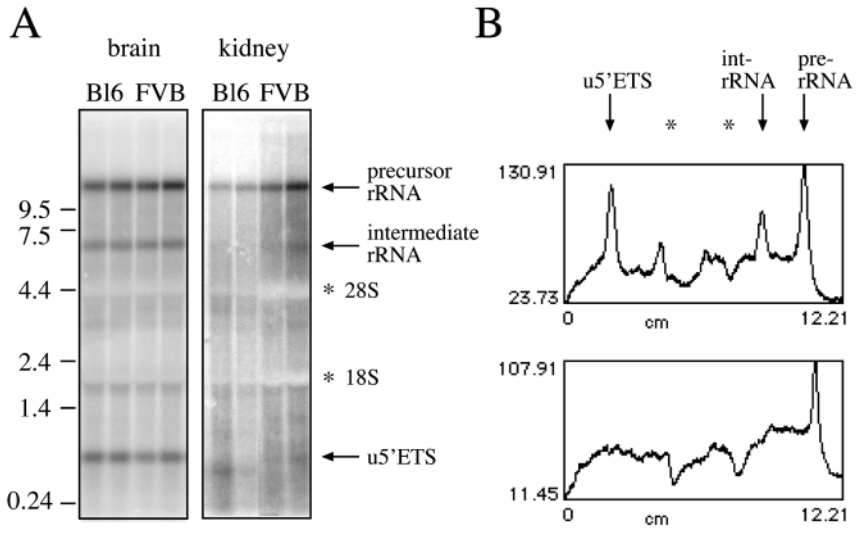

Fig. 1. Ribosomal RNA processing in mouse brain and kidney. (A) Total RNA, isolated from brain and kidney of two mice of the inbred FVB and Bl6 strains, was blotted and hybridised with the u5′ETS probe, depicted in Fig. 2A. RNA markers are indicated to the left. The positions of precursor (13 kb) and intermediate (6.6 kb) rRNAs, the u5′ETS fragment (0.6 kb) and of the mature 18S and 28S rRNAs (asterisks) are indicated to the right. Sizes of the different rRNAs were calculated using the RNA standards. (B) Densitometric analysis of the second lane of the brain (upper panel) and kidney (lower panel) RNA blots reveals that the intermediate and u5′ETS rRNAs are present in the brain but not detectable in kidney. Scans were generated from PhophorImager files, using NIH Image software. These data suggest that ribosomal RNA processing in the mouse brain differs from that in kidney.

cleaved 600 bp 5′ETS processing product. The finding of a 6.6 kb processing intermediate in the brain, indicates that an alternative rRNA processing pathway exists in this tissue, in which a site between 18S and 5.8S rRNAs (i.e. 6.6 kb downstream of the transciption inititaiton site) is cleaved first, instead of the 600 bp site at the 5′end of the rRNA precursor. Such an alternative pathway for pre-rRNA processing exists in *Xenopus laevis* (Rivera-Leon and Gerbi, 1997). Densitometric analysis of the northern blot in Fig. 1A confirmed that the 600 bp and 6.6 kb fragments are much more abundant in brain than in kidney (Fig. 1B). These data suggest that pre-rRNA processing in the murine brain is different from that in cultured cells or kidney, and that the 600 bp 5′ETS fragment is more stable in brain than in cultured cells. Therefore, when used in FISH experiments in the brain, the u5′ETS probe will detect sites of pre-rRNA processing in addition to sites of transcription.

Using the u5′ETS as a probe, we isolated several rDNA-containing cosmid clones (Fig. 2A). When tested by in situ hybridisation to metaphase spreads of mouse chromosomes, these cosmids produce highly specific signals. As shown in Fig. 2B, in the inbred FVB mouse strain, four rDNA loci are detected, which are all located near the centromere. Double labelling studies with chromosome specific telomere probes (data not shown), revealed that in FVB mice the rDNA loci are on chromosomes 12, 15, 18 and 19. FVB mice therefore resemble the inbred C57BL/10J, SJL/J and SWR/J mouse strains in the number of rDNA containing chromosomes and in the chromosomal localisation of these rDNA clusters (Kurihara et al., 1994).

On metaphase spreads, identical results were obtained with probes, corresponding to the rRNA precursor (transcribed sequence, or TS), or with probes, derived from the non-transcribed spacer (NTS; data not shown). Also in paraffin embedded mouse brain sections the TS and NTS probes produce almost identical signals (Fig. 2C-E), which are highly specific for the nucleolus (encircled in Fig. 2E, see also Figs 3, 5 and 6). These results demonstrate that both TS and NTS probes specifically detect rDNA, in spite of the fact that in particular the NTS probe contains many repeated sequences, that are also present in other regions of the mouse genome.

Combined RNA/DNA FISH reveals a pool of inactive rDNA in neurons

In control FISH experiments with the u5′ETS probe, no signal is observed on RNAse-pretreated mouse brain sections (results not shown), while a clear nucleolar signal is obtained in sections

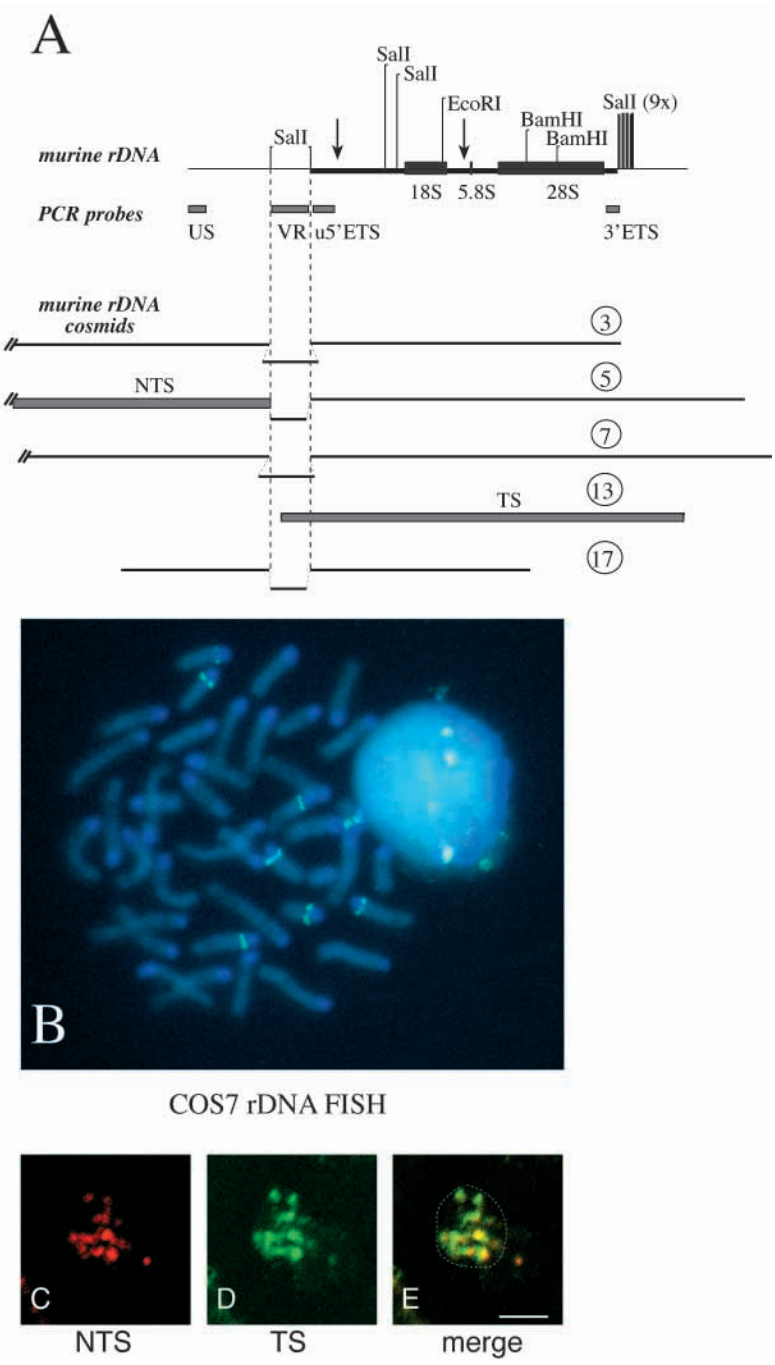

Fig. 2. Characterization of murine rDNA probes for FISH analysis. (A) Schematic representation of the 22 kb sequenced region of the murine rDNA repeat (accession number X82564). Precursor (thin black bar), 18S, 5.8S and 28 S rRNAs (thick bars) and some of the restriction enzyme sites within this region are indicated. Vertical arrows mark the approximate positions of putative processing sites in the pre-rRNA, as deduced from Fig. 1. The position of 5 rDNA containing cosmids, with respect to the 22 kb murine rDNA sequence is indicated. The position of the PCR probes used to characterize and map the cosmids is shown. Note the different variable repeat-regions in the cosmids. NTS: non-transcribed spacer; TS: transcribed sequence; US: upstream sequence; ETS: external transcribed spacer; VR: variable repeat. (B) FISH analysis on FVB mouse chromosomes, using biotinylated cosmid 7 as a probe reveals the presence of 4 rDNA loci in this inbred strain of mice. (C-E) FISH analysis on microwave treated, paraffin embedded mouse brain section using the NTS (red, C) and TS (green, D) probes depicted in A. Pictures were taken using a confocal laser scanning microscope. In E the green and red signals are merged. The nucleolus of a large neuron in the hypothalamus is depicted here (encircled in E). Notice the specific and largely overlapping hybridisation pattern obtained with both rDNA probes. Bar, 3 μm.

in which RNA is preserved, indicating the u5′ETS probe specifically detects rRNA transcripts. For detecting rDNA we used the NTS probe, which produces no signal on non-denatured tissue sections under RNA-FISH conditions (data not shown), while, as shown in Fig. 2C, this probe specifically labels nucleolar rDNA under DNA-FISH conditions. Therefore, double localisation studies, using first the u'5ETS probe for pre-rRNA detection, followed by the NTS probe for rDNA detection, were next performed on transverse sections of mouse brain, to analyse ribosomal gene transcription in the central nervous system. The cerebellum was chosen as a model system, because transcriptionally active Purkinje cells are positioned next to the granule cells, which have a low metabolic (and hence a low ribosomal gene) activity. As shown in Fig. 3A, the intensity of the u5′ETS staining is much higher in nucleoli of Purkinje cells (indicated by arrowheads), than in granule cells (of which some are encircled), reflecting the differential transcriptional activity in the two cell types. In addition, in Purkinje cells the probe is detected throughout the nucleolus, whereas in granule cells staining is restricted to small dots, of which 1-3 appear to be present per cell. The rRNA FISH contrasts with the rDNA staining shown in Fig. 3B, which is of a similar intensity in Purkinje and granule cells, due to the equal amounts of rDNA per cell.

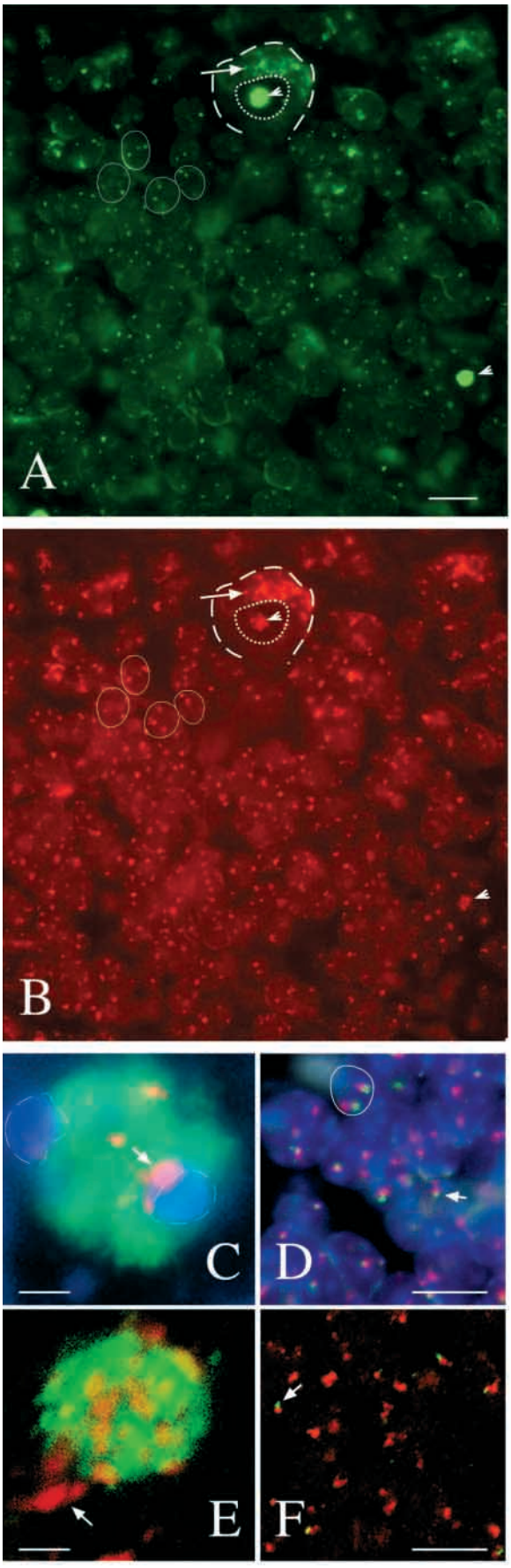

Fig. 3. Transcriptionally active and inactive ribosomal DNA. (A,B) Paraffin embedded, transverse sections of 5 μm through an adult mouse brain, were incubated with the u5′ETS probe (green signal for pre-rRNA detection), followed by the NTS probe (red signal for rDNA distribution), in a combined RNA/DNA FISH protocol. After detection with secondary antibodies sections were mounted in medium containing DAPI, to allow detection of heterochromatic regions of the nucleus. In A and B a low power magnification of part of the cerebellum is shown, as observed with normal epifluorescence, to demonstrate pre-rRNA (A) and rDNA (B) signals and the specificity of the combined FISH protocol. In this section, two Purkinje cell nucleoli are detected (arrowheads), which light up very strongly with the rRNA probe but much less so with the rDNA probe. The nuclear (dotted circle) and cytoplasmic (dashed circle) boundaries of one of the Purkinje cells have been indicated to demonstrate the cytoplasmic autofluorescence (arrow in A,B), which is visible through all filters (DAPI picture is not shown here). To aid in their identification, four granule cells have been encircled, to the left of the upper Purkinje cell. Notice the speckled pattern of hybridisation in this layer of the cerebellum, due to the fact that multiple, small nucleoli exist per granule cell. Bar in A, 10 μm. (C-F) Higher magnification of the large nucleoli of a Purkinje cell (C) and brainstem (E) neuron and of the small nucleoli of the granule cells (D,F), after a combined RNA/DNA FISH. Signals are merged to show colocalisation (or the lack of it) of pre-rRNA and rDNA. In C,D a normal epifluorescent microscope was used to capture the signals, in E,F a confocal microscope. Therefore, only in C,D the DAPI signal could be added (blue/purple signal), to produce a triple overlay. Notice the large red rDNA aggregates, indicated by arrows in C,E, which are devoid of rRNA signal and are located at the boundaries of the large nucleoli. These aggregates are likely to be transcriptionally inactive rDNA repeats. In C it is clear that this rDNA is adjacent to the DAPI-positive heterchromatin. In the granule cells (D,F), the rRNA signal (green) is always adjacent to and/or partially overlapping with the rDNA (NTS probe, red). Not all nucleolar organising regions express rRNA, in line with the fact that these cells have a low metabolic activity. In D, the DAPI overlay (blue) was enhanced to indicate cell nuclei, one of these is outlined. Bars: 1 μm (C,E); 10 μm (D,F).

At higher magnification (Fig. 3C,E), the FISH results suggest that in many neurons with a single large nucleolus, such as Purkinje cells of the cerebellum, the rDNA forms concentrated large aggregates and several smaller dots (see also Fig. 2C-E). When the rRNA/rDNA signals are superimposed and investigated either by normal epifluoresence microscopy (Fig. 3C), or with a confocal laser scanning microscope (Fig. 3E), it appears that the very large lumps of rDNA, that are located at the boundary of the nucleolus, in the vicinity of centromeric aggregates, are devoid of rRNA signal (see arrows in Fig. 3C,E). Therefore, this fraction of the rDNA pool likely represents clusters of inactive rDNA genes. The lumps do not overlap with the heterochromatic ring, as judged from a triple overlay with DAPI (Fig. 3C, the DAPI stained area is encircled).The data suggest that many of the inactive rDNA genes are attached to the periphery of the large neuronal nucleolus, but they do not merge with nuclear heterochromatin and thus seem to form a distinct domain of inactive DNA. Such an organisation is not specific for Purkinje cells, but is observed in many types of large neurons with a single nucleolus. In granule cells, on the other hand, the transcription signal (in green) is generally found on the tip of the rDNA signal (in red), of which several dots per nucleus occur (Fig. 3D,F). These data indicate that in granule cells only a very small number of selected rDNA genes are active, which are likely to form the small nucleoli present in these cells (Peters et al., 1991).

Transcriptionally inactive rDNA is methylated, but contains little MeCP2

The combined RNA/DNA FISH data suggest that an inactive rDNA fraction exists in the nucleoli of large neurons, which forms a distinct chromatin domain, located adjacent to the centromeric DNA inside the nucleolus. Since transcriptional inactivation is often associated with increased methylation at CpG-residues, we wanted to determine whether the inactive rDNA aggregates are methylated. To determine whether FVB rDNA repeats are methylated, we analyzed genomic DNA, digested with *Eco*RI, *Eco*RI and *Hpa*II (an enzyme, sensitive to methylation at CpG-residues in the context of CCGG), or *Eco*RI and *Msp*I (methylation-insensitive enzyme), by southern blot, using u5′ETS as a probe (Fig. 4A). As a control, DNA from a C57Bl6 mouse was taken, since in this mouse strain the rDNA repeats are practically devoid of methylation (Bird et al., 1981). To verify that the *Hpa*II digestion of the rDNA loci was complete, we reprobed the blot with an unrelated single copy gene probe, which contains an 8 kb *Hpa*II-resistant (i.e. methylated) fragment and a 4.3 kb *Hpa*II-sensitive band (Fig. 4B).

In *Eco*RI-digested DNA u5′ETS hybridises to large DNA fragments of >11kb. After *Eco*RI/ *Hpa*II digestion, three types of *Hpa*II-resistant fragments are detected in the brain DNA of FVB mice (Fig. 4A): the original *Eco*RI fragments (>11 kb); bands ranging in size between 6 and 9 kb (indicated by brackets in Fig. 4A), and a regularly spaced ladder of lower molecular mass bands. In the C57Bl6 mouse only the lower molecular mass bands are seen (Fig. 4A), which confirms the results that in this mouse strain the rDNA is not heavily methylated (Bird et al., 1981). All *Hpa*II-resistant fragments are digested by *Msp*I, suggesting that extensive methylation occurs throughout the rDNA repeat in FVB mice. The simplest explanation for these results is that in FVB mice some of the rDNA genes are methylated along the entire >11 kb *Eco*RI-region, giving rise to completely *Hpa*II-protected bands, while others are partially methylated, giving rise to the 6-9 kb products and to the low molecular mass ladder. These results support the recent proposal for the human rDNA genes, i.e. that a small proportion of these repeats is completely methylated (and may be constitutively silent), while the remainder is methylated in the non-transcribed region of the gene and not, or partially, methylated in the transcribed part (Brock and Bird, 1997). The number of completely methylated fragments is constant between littermates of the inbred FVB strain and using densitometric scanning it was estimated to be around 20% (data not shown).

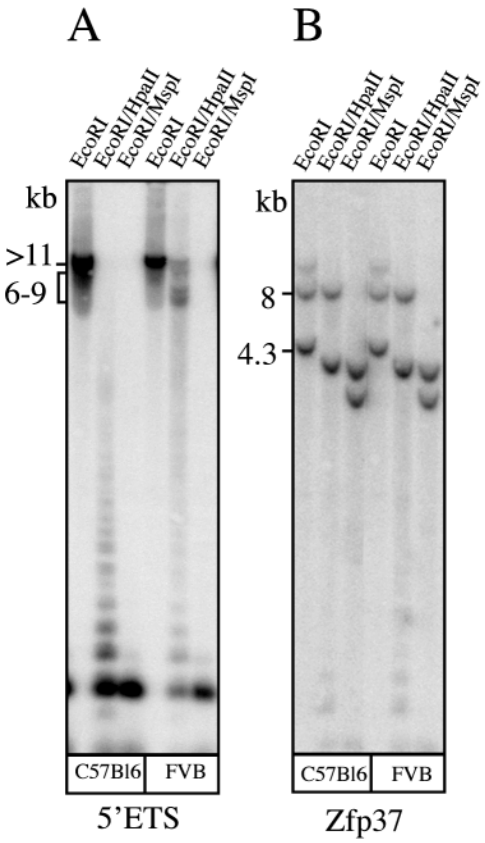

Fig. 4. Methylation of the rDNA repeats in FVB mice. Genomic DNA, isolated from the brain of one C57Bl6 or of one FVB mouse, was digested with *Eco*RI, *Eco*RI and *Hpa*II, or *Eco*RI and *Msp*I, electrophoresed and blotted. The southern blot was first hybridised with the u5′ETS probe (A), depicted in Fig. 2A. After washing the blot was exposed to a PhosphorImager screen to detect radioactive signals. The blot was subsequently stripped and rehybridised with a probe specific for the murine Zfp37 gene (B). Notice that some of the rDNA hybridisation is still visible in B, due to the strong signal obtained with the rDNA repeats. Lengths (in kb) of bands, recognised by the two probes, are indicated to the left.

Since FVB rDNA is methylated, we next tested whether in neurons the methylated rDNA can be distinguished in situ, using anti-5-methylcytosine (5MC) monoclonal antibodies in conjunction with rDNA FISH. These immuno-FISH studies were possible on tissue sections because we treated them with the microwave in order to retrieve antigen and to denature nucleic acids. The 5MC signal is largely restricted to the

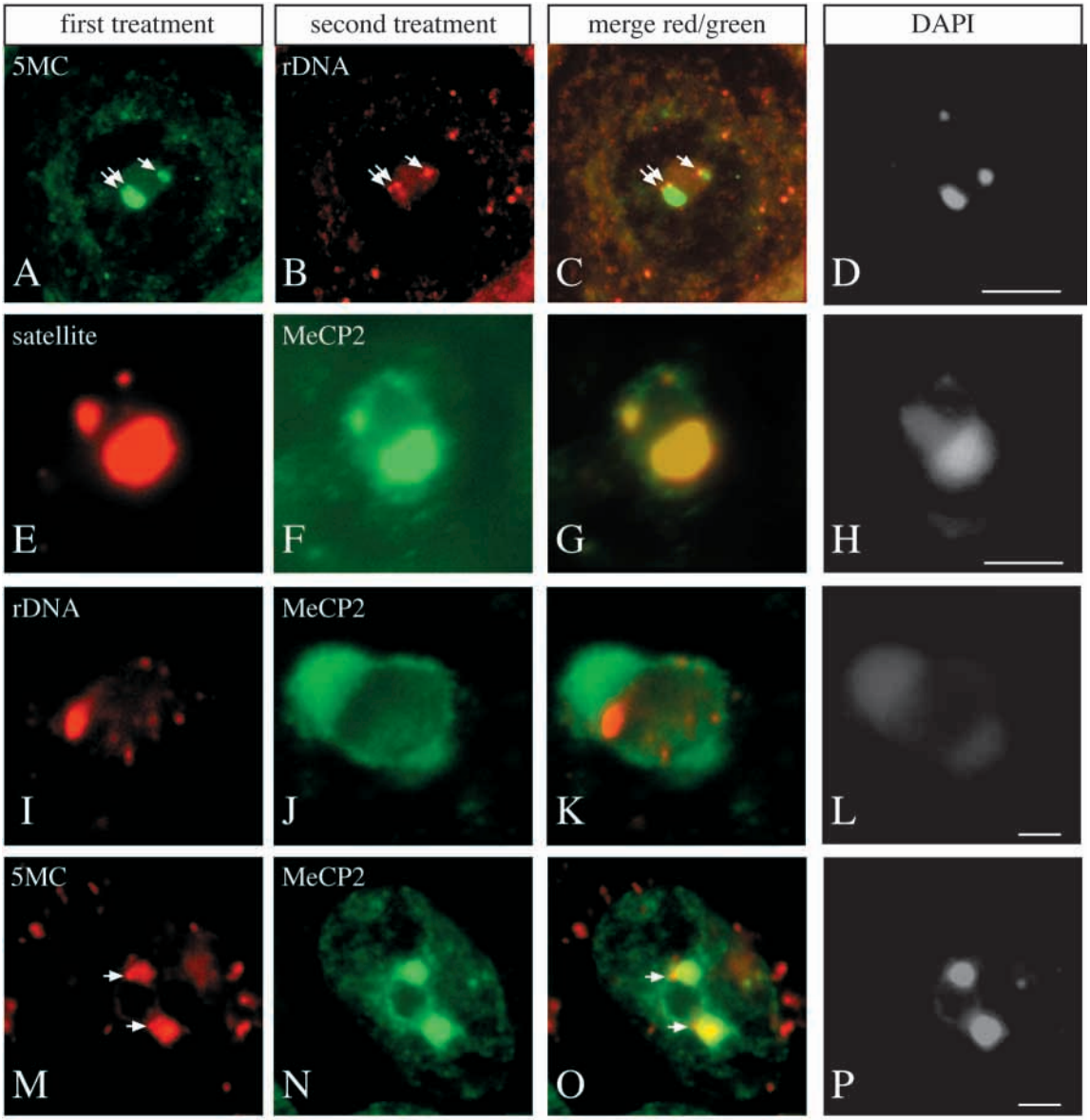

Fig. 5. Characterization of the inactive rDNA fraction in nucleoli of large neurons. Transverse sections of 5 μm, cut through the brain of an adult FVB mouse, were analyzed for the colocalisation of 5-methylcytosine residues (5MC), the methylated DNA binding protein MeCP2, rDNA or centromeric DNA, using a combined immuno-FISH protocol. First and second treatment refers to the sequence of events in this combined protocol. After completion of the experiments, sections were mounted in medium with DAPI, of which the staining pattern is shown (in black and white) in the last column. (A-D) Colocalisation of 5MC (green, A) and rDNA (red, B). The 5MC antibodies localise mainly to centromeric DNA, as judged with the DAPI stain (D). This correlates with the fact that mouse centromeric DNA is heavily methylated. Adjacent to this region of 5MC concentration, there are small domains, indicated by arrows, that are outside the DAPI-positive material, but that colocalise with rDNA, as is seen in the overlay. Bar, 3 μm. (E-H) Colocalisation of γ-satellite DNA (red, E) and MeCP2 (green, F). The satellite probe brightly marks centromeric DNA, but not the MeCP2-positive perinucleolar heterochromatin ring, showing that these two types of heterochromatin have a different DNA-composition. Bar, 2.5 μm. (I-L) Immuno-FISH of rDNA (red, I) and MeCP2 (green, J). Notice that MeCP2 does not colocalise with the large inactive rDNA fraction, as shown in an overlay picture (K). Bar, 2 μm. (M-P) Colocalisation of 5MC (red, M) and MeCP2 (green, N). These antibodies label highly similar areas of the neuronal nucleus, including the centromeres, but the spots that represent inactive rDNA repeats (arrows) are labeled with 5MC antibodies only. These results indicate that a fraction of the inactive rDNA genes is methylated but not abundantly decorated with MeCP2. Bar, 4 μm.

centromeric DNA attached to the nucleolus, as judged by comparison to the DAPI staining (Fig. 5A,D), consistent with the fact that centromeric DNA in mice is heavily methylated. However, in addition to the strong centromeric staining, small dots of 5MC signal are also visible adjacent to the centromeres (see arrows in Fig. 5A-C). These dots stain both with the 5MC antibodies, as well as with the rDNA probe (Fig. 5A-C). In contrast to these intense signals the remainder of the nucleolus is only weakly stained by the 5MC antiserum. These data suggest that an rDNA fraction exists inside the large nucleoli of FVB neurons, that is methylated to a higher extent than the remainder of the nucleolar rDNA and which is located adjacent

to centromeric DNA. Strikingly, this methylated rDNA pool occupies the same position as the transcriptionally inactive rDNA described in Fig. 3, indicating that these pools represent the same fraction of rDNA.

As the transcriptionally inactive rDNA fraction appears to be methylated more densely, we analyzed whether this rDNA is bound by MeCP2, since this protein has been shown to bind to methylated, transcriptionally silent regions of the genome. Moreover, MeCP2 is highly enriched in the brain (Nan et al., 1997) and was shown to colocalise with DAPI-positive, heterochromatic regions surrounding the nucleolus (Payen et al., 1998). Using a γ-satellite oligonucleotide probe (which should localise to the centromeres) in a combined immuno-FISH experiment with anti-MeCP2 antibodies, we first ascertained that the MeCP2 distribution is not altered by the immuno-FISH procedure. Indeed, as shown in Fig. 5E-H, the MeCP2 antibodies still colocalise with the DAPI-positive signal and with the γ-satellite probe after the immuno-FISH. In addition, the anti-MeCP2 antiserum also stains the heterochromatin rim surrounding the nucleolus, which is devoid of γ-satellite. The results with the γ-satellite oligonucleotide are in agreement with a previous in situ hybridisation, using nick translated satellite DNA and peroxidase staining methods (Manuelidis, 1984b) and indicate that perinucleolar heterochromatin is distinct in its DNA sequence content from centromeres. Together the results suggest that the immuno-FISH protocol does not affect MeCP2 distribution in a detectable manner.

When the MeCP2 distribution is tested in conjunction with an rDNA FISH, it is clear that MeCP2 does not colocalise significantly with the rDNA (Fig. 5I-L). Similarly, when the anti-5MC and anti-MeCP2 antisera are used in a double labelling experiment, they overlap to a great extent in the centromeric chromatin regions, but not in the punctate regions that were shown to contain inactive rDNA (Fig. 5M-P). Taken together these data indicate that in FVB mouse neurons MeCP2 is distributed over methylated DNA sequences, with the notable exception of the transcriptionally inactive and methylated rDNA fraction.

Identification of novel neuronal nuclear domains, enriched in transcriptional repressors

Like MeCP2, histone H1 is a factor associated with transcriptionally inactive DNA (Zlatanova and Yaneva, 1991). We therefore tested whether this protein is detected on the inactive rDNA pool in neurons. For this assay we examined large brainstem neurons, since histone H1 is virtually absent from Purkinje cells (Garcia-Segura et al., 1993; Payen et al., 1998). The combined immuno-FISH results suggest that

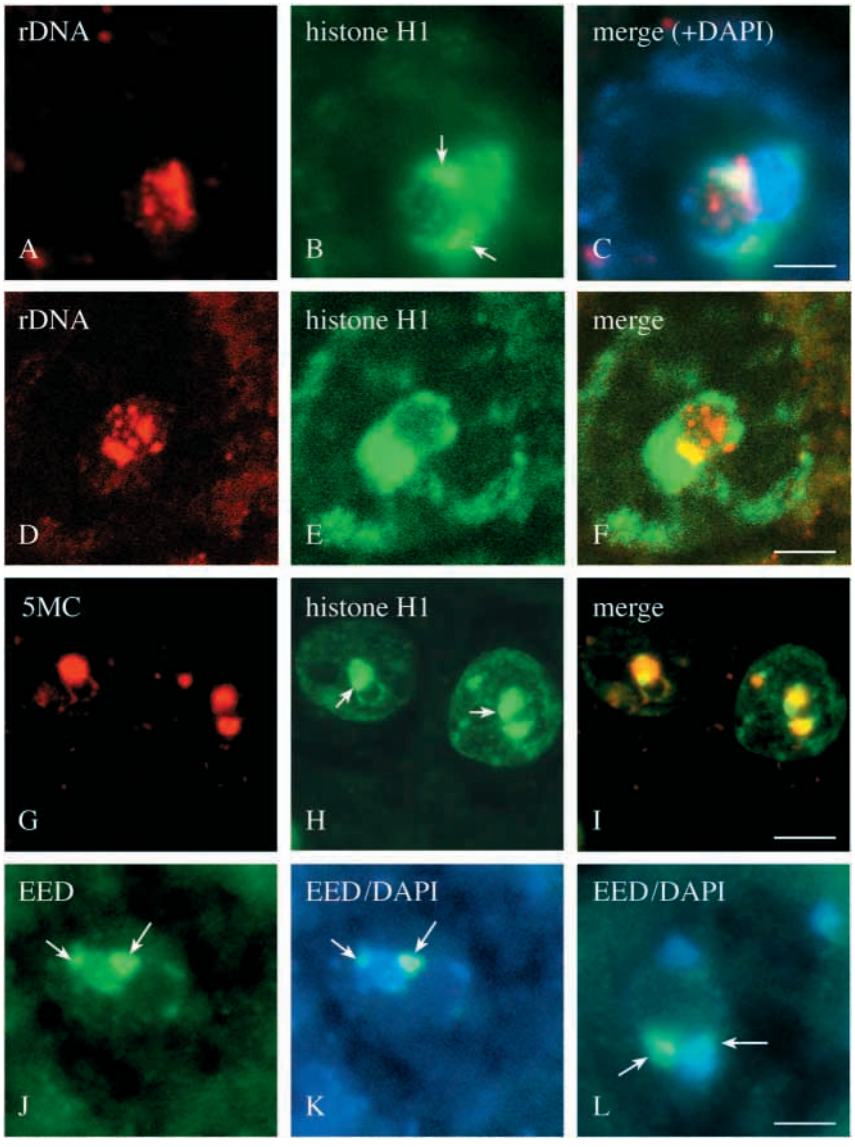

Fig. 6. Histone H1 and Eed distribution in neurons. (A-I) To investigate whether histone H1 is present in the inactive, methylated rDNA fraction, colocalisation experiments with rDNA (red, A,D) and anti-histone H1 antiserum (green, B,E), or with 5MC (red, G) and histone H1 (green, H) antibodies, were carried out on transverse sections of mouse brain. In A-C and G-I an epifluorescent microscope was used to capture the signals, in D-F a confocal microscope. In C, the triple stain with DAPI is shown, in F and I the overlay of red and green only. In the neuronal nuclei with a single large nucleolus, the histone H1 signal partially overlaps with that of the rDNA, but histone H1 is also detected in distinct pericentromeric domains, that remain green in the overlay and that are indicated by arrows. Bar, 5 μm. In the colocalisation of 5MC with histone H1 two nuclei are visible (G-I), both of which contain 5MC- and H1-positive centromeric DNA, as well as pericentromeric areas, rich in histone H1 but not in 5MC (arrows). (J-L) Localisation of the polycomb group protein Eed. A similar pericentromeric heterochromatic domain, as seen with the histone H1 antibodies, is stained with a polyclonal antiserum against Eed (green). In J,K one nucleolus is depicted, stained with anti-Eed only (J), or with anti-Eed and DAPI (K). In L the anti-Eed overlay with DAPI is shown on a different nucleolus. The data demonstrate that Eed stains centromeric and pericentromeric heterochromatin. Bar, 2 μm.

histone H1 is present in the centromeric heterochromatin, on the perinucleolar rim and that it overlaps partially with the rDNA domains (Fig. 6A-F). Thus, histone H1 associates with the inactive rDNA fraction. However, histone H1 is also prominently detected in distinct subdomains (arrows in Fig. 6B), which are adjacent to the rDNA signal and attached to centromeric heterochromatin and/or the perinucleolar rim. These neuronal histone H1-rich domains could be detected with two independent antibody preparations (data not shown). Judging from colocalisation experiments, these novel domains do not contain γ-satellite DNA (data not shown), and no high concentration of 5MC (Fig. 6G-I). This pattern of histone H1 distribution is in sharp contrast to the uniform labelling with anti-histone H1 antibodies, observed in different cultured cell types (Parseghian et al., 1993; data not shown).

Remarkably, an antiserum against the mammalian Polycomb group protein Eed also appears to detect these 'H1-domains', which are clamped between the centromeric blobs and perinucleolar heterochromatin (Fig. 6J-L, arrows). Since also Eed protein was reported to be uniformly distributed in cultured cell nuclei (Sewalt et al., 1998; van Lohuizen et al., 1998), its concentration in pericentromeric chromatin domains appears to be specific for neurons.

Distribution of coilin in microwave treated, paraffin embedded neurons

A number of markers, used in this study, such as histone H1, MeCP2 and 5MC, display staining of the DAPI-positive heterochromatin rim, surrounding the nucleolus. On the other hand, previous studies in the rat brain and in cultured neurons identified a perinucleolar cap structure (also termed 'rosette'), which occupies a very similar position in neuronal nuclei and which is stained by coilin antibodies (Lafarga et al., 1998; Santama et al., 1996). To determine the relationship between the 'rosette' and perinucleolar heterochromatin, we performed colocalisation studies with the 5MC- and coilin-specific antibodies. In Fig. 7 two optical sections through a single neuron, taken with the use of a confocal microscope, are shown. In the first section a rounded structure is detected (Fig. 7A, arrow), which is located near to the nucleolus and very likely represents a Cajal (or coiled) body. In the other section (Fig. 7D) the typical perinucleolar 'rosette' staining of coilin is visible (marked by arrowheads). The 5MC- and coilin positive structures are interspersed, but overlap only slightly (Fig. 7E,F). These data indicate that cytologically distinct domains, enriched in components of either the transcriptional repression machinery or of RNA processing complexes are asscociated with the nucleolar surface. The results in Fig. 7 agree with the previous studies on coilin distribution in rat neurons (Lafarga et al., 1998; Santama et al., 1996) and present further evidence that the harsh treatment of paraffin embedded sections of the brain, as described here, still allows good preservation of intranuclear structure.

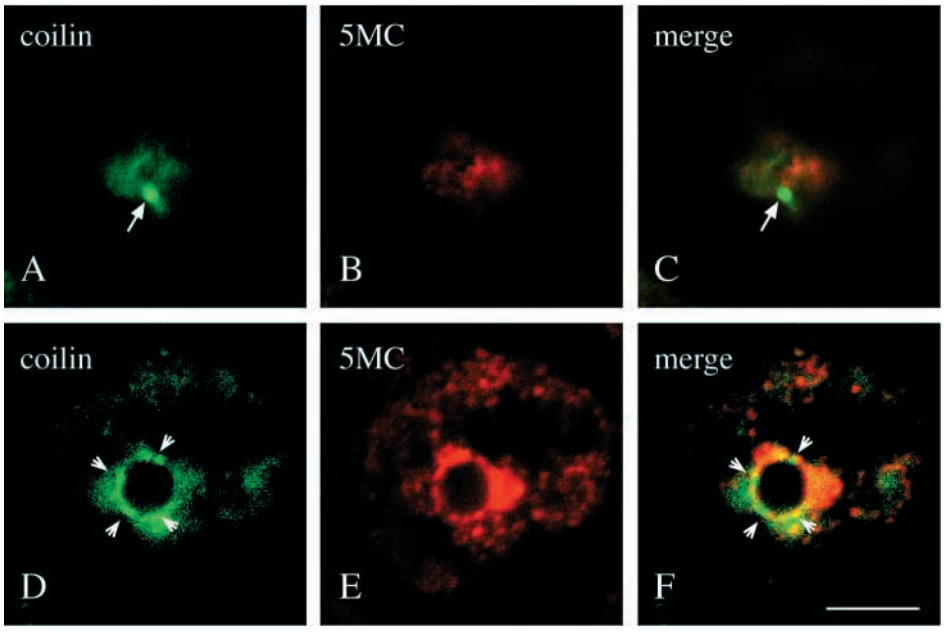

Fig. 7. Coilin and 5MC localisation in large neurons. Double labelling on a large neuron using polyclonal anti-coilin antibodies (A,D, green) and anti-5MC antiserum (B,E, red). Images were acquired with a confocal microscope. Two sections through the same neuron are shown. In A-C, a section above the nucleolus demonstrates the presence of coilin in a round structure, which very likely represents a Cajal body. In D-F, a section through the nucleolus demonstrates the cap-like perinucleolar staining with the anti-coilin antibodies (arrowheads). Notice that coilin and 5MC distributions are mostly nonoverlapping (merges in C,F).

DISCUSSION

In this report we describe a modified procedure for combined FISH/immunofluorescence, which allows simultaneous detection of RNA and DNA, or the detection of nucleic acid sequences with nuclear proteins, on paraffin-embedded sections of mouse brain. Using this method we have examined the nuclear architecture of neurons. Since the organisation of the nucleus and the number and appearance of various nuclear bodies display a great degree of variation in different cell culture systems, the importance of studying tissue material, which represents the actual in vivo situation, should not be underestimated. Paraffin embedding of tissue allows good preservation of the three-dimensional nuclear structure, but reduces the sensitivity of in situ hybridisation and immunocytochemistry. Microwave treatment of the samples helps to overcome the latter problem without significantly disrupting nuclear structure, since the distribution of markers, such as γ-satellite DNA and coilin, observed in our experiments, is similar to that described previously (Lafarga et al., 1998; Manuelidis, 1984b).

Using the combined FISH/immunofluorescence protocol, we describe the existence of four classes of chromatin in large neurons, which are intimately associated with the nucleolus: (1) centromeric DNA; (2) a ring of perinucleolar

heterochromatin; (3) inactive rDNA and (4) pericentromeric Eed and/or H1 positive domains. A summary of the data is presented in Fig. 8, in a model of the transcriptionally active and inactive chromatin domains found in large neurons. The presence of the first two classes of chromatin near neuronal nucleoli has been reported in a number of studies, but the latter two domains have not been noted yet. Previous reports did show that in neurons transcriptionally inactive DNA, including the inactive X-chromosome (Borden and Manuelidis, 1988) and a large inactive DNA repeat of several megabases (Manuelidis, 1991), are associated with centromeric heterochromatin and the nucleolus. The novel perinucleolar H1/ Eed-positive domains reported here are also likely to represent transcriptionally silent DNA, since Eed protein has been shown to associate with histone deacetylases and repress transcription in a number of assays (van der Vlag and Otte, 1999). We show that also *inside* nucleoli inactive DNA, consisting of methylated ribosomal genes, assembles adjacent to the perinucleolar heterochromatin. These data underscore the intricate relationship between heterochromatin and inactive rDNA (Carmo-Fonseca et al., 2000). Thus, our studies extend previous experiments and emphasise that large neurons with a single nucleolus have an organisation of heterochromatin around their nucleolus that appears to separate RNA polymerase II- (and III-) transcriptional domains from RNA polymerase I-domains.

The localisation of an inactive rDNA fraction to a region adjacent to the centromere, made it possible to determine what proteins bind to this type of chromatin. MeCP2, which belongs to a small family of proteins containing a conserved methylated CpG-binding domain, or MBD (Hendrich and Bird, 1998), was an excellent candidate for binding to inactive rDNA. This protein was shown to bind methylated DNA in vitro, to localise to methylated regions of the genome and to be highly abundant in brain tissue (Nan et al., 1997; Nan et al., 1993; Nan et al., 1996). Furthermore, recent studies have shown that MeCP2 can interact with histone deacetylases and in this way promote transcriptional repression (Jones et al., 1998; Nan et al., 1998). However, although inactive rDNA clusters appear to be methylated and accessible to antibodies, we could not detect a significant association of MeCP2 with these clusters. In the same cells, MeCP2 is quite abundant within other methylated chromatin structures, such as the aggregates of centromeres and the perinucleolar heterochromatic ring. This observation provides a direct indication that MeCP2 is not randomly distributed over methylated CpG sites, but is selectively excluded from methylated inactive rDNA. Perhaps the association of MeCP2 with TFIIB, a component of the RNA polymerase II complex (Kaludov and Wolffe, 2000), underlies this exclusion. Alternatively, it could be achieved by sequence-specific DNA binding proteins that are involved in rDNA inactivation. It will be interesting to determine whether any of the other recently characterized MBD-containing proteins bind to the inactive rDNA population. In addition, it will be of interest to examine whether in other cell types MeCP2 is excluded from inactive rDNA.

Histone H1, a linker histone implicated in transcriptional repression (Zlatanova and Yaneva, 1991), was shown to have a repressing effect on the 5S ribosomal genes in vivo (Bouvet et al., 1994). There is controversy over whether histone H1 mediates repression through preferential binding to methylated DNA (Bird and Wolffe, 1999; Campoy et al., 1995; McArthur and Thomas, 1996). Here we show that histone H1 associates with the inactive methylated rDNA fraction, but is hardly detected in the remainder of the nucleolus, in spite of the fact that both domains are occupied by the same DNA sequences. Although one could explain our observations by assuming that histone H1 is excluded from the actively transcribing regions of the nucleolus, our data indicate that in the case of the rDNA genes, histone H1 does have a preference for the more methylated DNA fraction.

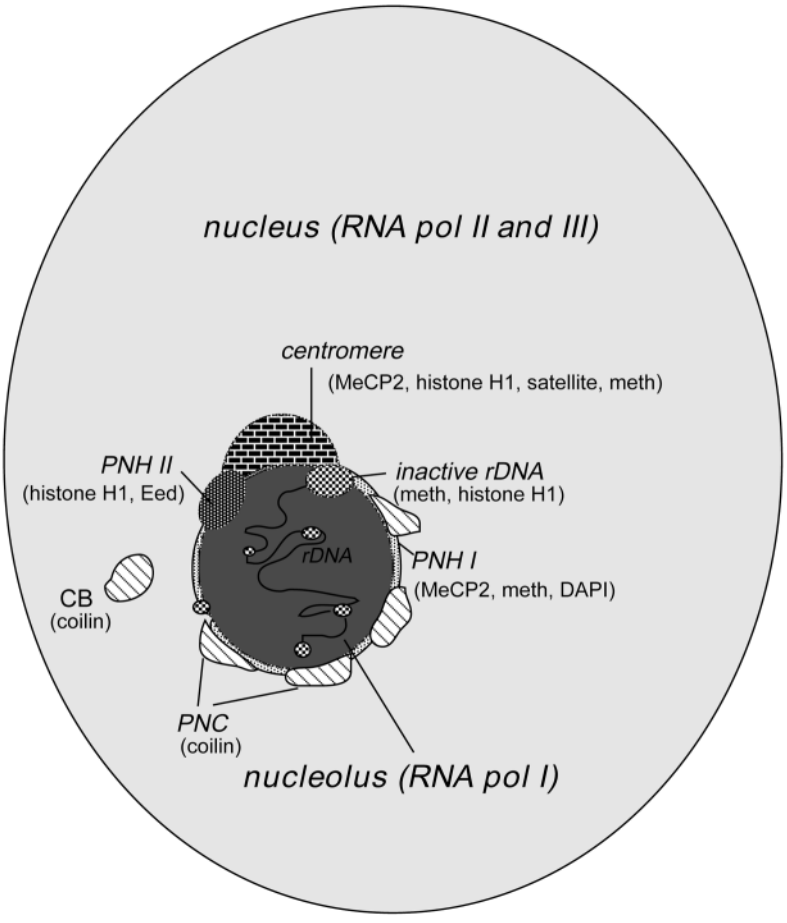

Fig. 8. Neuronal nuclear and nucleolar chromatin domains. Transcriptionally active and inactive chromatin domains in an FVB neuron. This schematic overview summarises the data described here and obtained by other groups. The single large nucleolus of this neuron is surrounded by a heterochromatic shell, to which several distinct, inactive DNA domains are attached, both to the outside as well as to the inside of the nucleolus. The protein and DNA composition of each domain is indicated. The heterochromatin ring thus serves as an attachment site for inactive DNA. CB: Cajal body; meth: methylated DNA; PNH I and –II: perinucleolar heterochromatin domain I and –II; PNC: perinucleolar cap (also called ‘rosette’).

The fact that the inactive rDNA fraction, adjacent to perinucleolar heterochromatin, is highly methylated, strongly suggests that also in the rDNA genes methylation and transcriptional repression are intimately linked processes. However, methylation can only explain part of the inactivation of rDNA genes in any given cell type, since the methylation patterns of the rDNA genes appear to be set early in development and they do not differ between rDNA isolated from different tissues (Bird et al., 1981), while rDNA activity does differ drastically between cells from different tissues, as we have shown here for granule cells of the cerebellum and Purkinje cells. It is tempting to speculate that the perinucleolar, methylated and inactive rDNA fraction represents (part of the) constitutively inactive rDNA genes, which were proposed to exist in the case of human rDNA genes (Brock and Bird, 1997). The remainder of the rDNA genes are distributed within the nucleolus, in a thread-like pattern, containing a number of knots (see Figs 2, 3, 5, 6). These might represent the active and facultative inactive population of rDNA genes, which is less methylated and appears to contain little or no MeCP2, or histone H1.

Neurons are postmitotic cells and absence of DNA replication and chromosome segregation would allow the establishment of stable nuclear structures that correspond optimally to the requirements of transcription and RNA processing. The difference in chromatin organisation of neurons compared to that of dividing cells is underscored by the distribution of histone H1. This highly abundant nuclear protein displays a more uniform distribution in cultured cells than in large neurons, where it is expressed at lower levels and predominantly associated with centromeric chromatin and pericentromeric chromatin domains. The latter domains appear to be enriched in a PcG protein Eed. It is noteworthy that in previous in situ hybridisations on human brain, a repetitive probe localising to the large pericentromeric region on chromosome 1q12, also showed a preferential localisation adjacent to neuronal centromeric DNA (Arnoldus et al., 1989). A complex of mammalian PcG proteins (RING1, BMI1, hPc2) was shown to specifically bind to this repetitive sequence to form a novel nuclear domain in cultured cells (Saurin et al., 1998). However, it is unlikely that the Eed positive domains identified by us in mouse neurons correspond to the human PcG-binding pericentromeric region 1q12, because Eed does not interact biochemically with the PcG complex which includes the proteins mentioned above, and it does not colocalise with these proteins in cultured cells (Sewalt et al., 1998; van Lohuizen et al., 1998). Since in dividing cells Eed, as well as histone H1, shows a much more homogeneous distribution, an attractive possibility is that small transcriptionally inactive domains, containing Eed and rich in histone H1, which are randomly localised in dividing cells, are associated around the centromeric heterochromatin and nucleolus in neurons. DNA replication and/or cell division might disrupt such association, while it can proceed to completion in neurons, where none of these processes takes place.

In yeast, RNA polymerase II-transcribed reporter genes, integrated within an rDNA locus, undergo transcriptional silencing (Smith and Boeke, 1997). It is thought that this suppression serves to protect the rDNA repeats against illegitimate recombination. Silencing is mediated by the complex of Sir proteins, which is redistributed from the telomeres to the nucleolus, to suppress the generation of extrachromosomal rDNA circles, which cause aging in yeast (Sinclair and Guarente, 1997). Whether similar mechanisms play a role in aging in vertebrates needs to be shown, but it is possible that aberrant polymerase II activity within the nucleolus and DNA repair processes associated with it could promote recombination between tandem rDNA repeats and thereby promote aging. Such processes would have extremely serious consequences, especially in cells with very long life span and high proportion of active rDNA repeats, such as neurons. Thus, the strict separation of transcriptional domains described here could reflect the necessity to maintain high levels of pre-rRNA transcription without deleterious effects on the structure of the rDNA genes.

We thank all colleagues that generously send aliquots of their antibody preparations. We also thank B. Eussen (Dept of Clinical Genetics, Erasmus University) for his help with setting up the in situ hybridisations. This research was supported by the Royal Dutch Academy of Arts and Sciences (KNAW) and the Life Sciences Foundation (SLW; 803.33.311).

REFERENCES

Arnoldus, E. P., Peters, A. C., Bots, G. T., Raap, A. K. and van der Ploeg, M. (1989). Somatic pairing of chromosome 1 centromeres in interphase nuclei of human cerebellum. *Hum. Genet.* **83**, 231-234.

Auffray, C. and Rougeon, F. (1980). Purification of mouse immunoglobulin heavy-chain messenger RNAs from total myeloma tumor RNA. *Eur. J. Biochem.* **107**, 303-314.

Bird, A. P., Taggart, M. H. and Gehring, C. A. (1981). Methylated and unmethylated ribosomal RNA genes in the mouse. *J. Mol. Biol.* **152**, 1-17.

Bird, A. P. and Wolffe, A. P. (1999). Methylation-induced repression – belts, braces, and chromatin. *Cell* **99**, 451-454.

Borden, J. and Manuelidis, L. (1988). Movement of the X chromosome in epilepsy. *Science* **242**, 1687-1691.

Bouvet, P., Dimitrov, S. and Wolffe, A. P. (1994). Specific regulation of Xenopus chromosomal 5S rRNA gene transcription in vivo by histone H1. *Genes Dev.* **8**, 1147-1159.

Brock, G. J. and Bird, A. (1997). Mosaic methylation of the repeat unit of the human ribosomal RNA genes. *Hum. Mol. Genet.* **6**, 451-456.

Campoy, F. J., Meehan, R. R., McKay, S., Nixon, J. and Bird, A. (1995). Binding of histone H1 to DNA is indifferent to methylation at CpG sequences. *J. Biol. Chem.* **270**, 26473-26481.

Carmo-Fonseca, M., Mendes-Soares, L. and Campos, I. (2000). To be or not to be in the nucleolus. *Nature Cell Biol.* **2**, E107-112.

Cockell, M. and Gasser, S. M. (1999). Nuclear compartments and gene regulation. *Curr. Opin. Genet. Dev.* **9**, 199-205.

Cook, P. R. (1999). The organization of replication and transcription. *Science* **284**, 1790-1795.

Denisenko, O. N. and Bomsztyk, K. (1997). The product of the murine homolog of the Drosophila extra sex combs gene displays transcriptional repressor activity. *Mol. Cell Biol.* **17**, 4707-4717.

Feinberg, A. P. and Vogelstein, B. (1983). A technique for radiolabeling DNA restriction endonuclease fragments to high specific activity. *Anal. Biochem.* **132**, 6-13.

Fourney, R. M., Miyakoshi, J., Day, R. S. and Paterson, M. C. (1988). Northern blotting: efficient RNA staining and transfer. *Focus* **10**, 5-7.

Garcia-Segura, L. M., Luquin, S., Martinez, P., Casas, M. T. and Suau, P. (1993). Differential expression and gonadal hormone regulation of histone H1(0) in the developing and adult rat brain. *Brain Res. Dev. Brain Res.* **73**, 63-70.

Gurney, T. Jr (1985). Characterization of mouse 45S ribosomal RNA subspecies suggests that the first processing cleavage occurs 600 +/- 100 nucleotides from the 5′ end and the second 500 +/- 100 nucleotides from the 3′ end of a 13.9 kb precursor. *Nucl. Acids Res.* **13**, 4905-4919.

Haaf, T., Hayman, D. L. and Schmid, M. (1991). Quantitative determination of rDNA transcription units in vertebrate cells. *Exp. Cell Res.* **193**, 78-86.

Hadjiolov, A. (1985). The nucleolus and ribosome biogenesis. In *Cell Biology*

Monographs, vol. 12 (ed. A. M. Beermann, L. Golstein, K. R. Porter and P. Sitte), pp. 1-263. Berlin Heidelberg New York: Springer.

Hendrich, B. and Bird, A. (1998). Identification and characterization of a family of mammalian methyl-CpG binding proteins. *Mol. Cell Biol.* **18**, 6538-6547.

Henikoff, S. (1998). Conspiracy of silence among repeated transgenes. *BioEssays* **20**, 532-535.

Jones, P. L., Veenstra, G. J., Wade, P. A., Vermaak, D., Kass, S. U., Landsberger, N., Strouboulis, J. and Wolffe, A. P. (1998). Methylated DNA and MeCP2 recruit histone deacetylase to repress transcription. *Nature Genet.* **19**, 187-191.

Kaludov, N. K. and Wolffe, A. P. (2000). MeCP2 driven transcriptional repression in vitro: selectivity for methylated DNA, action at a distance and contacts with the basal transcription machinery. *Nucl. Acids Res.* **28**, 1921-1928.

Kurihara, Y., Suh, D. S., Suzuki, H. and Moriwaki, K. (1994). Chromosomal locations of Ag-NORs and clusters of ribosomal DNA in laboratory strains of mice. *Mamm. Genome* **5**, 225-228.

Lafarga, M., Berciano, M. T., Garcia-Segura, L. M., Andres, M. A. and Carmo-Fonseca, M. (1998). Acute osmotic/stress stimuli induce a transient decrease of transcriptional activity in the neurosecretory neurons of supraoptic nuclei. *J. Neurocytol.* **27**, 205-217.

Lazdins, I. B., Delannoy, M. and Sollner-Webb, B. (1997). Analysis of nucleolar transcription and processing domains and pre-rRNA movements by in situ hybridization. *Chromosoma* **105**, 481-495.

Manuelidis, L. (1984a). Active nucleolus organizers are precisely positioned in adult central nervous system cells but not in neuroectodermal tumor cells. *J. Neuropathol. Exp. Neurol.* **43**, 225-241.

Manuelidis, L. (1984b). Different central nervous system cell types display distinct and nonrandom arrangements of satellite DNA sequences. *Proc. Nat. Acad. Sci. USA* **81**, 3123-3127.

Manuelidis, L. and Borden, J. (1988). Reproducible compartmentalization of individual chromosome domains in human CNS cells revealed by in situ hybridization and three-dimensional reconstruction. *Chromosoma* **96**, 397-410.

Manuelidis, L. (1991). Heterochromatic features of an 11-megabase transgene in brain cells. *Proc. Nat. Acad. Sci. USA* **88**, 1049-1053.

Mazarakis, N., Michalovich, D., Karis, A., Grosveld, F. and Galjart, N. (1996). *Zfp-37* is a member of the KRAB zinc finger gene family and is expressed in neurons of the developing and adult CNS. *Genomics* **33**, 247-257.

McArthur, M. and Thomas, J. O. (1996). A preference of histone H1 for methylated DNA. *EMBO J.* **15**, 1705-1714.

Miller, K. G. and Sollner-Webb, B. (1981). Transcription of mouse rRNA genes by RNA polymerase I: in vitro and in vivo initiation and processing sites. *Cell* **27**, 165-174.

Mulder, M. P., Wilke, M., Langeveld, A., Wilming, L. G., Hagemeijer, A., van Drunen, E., Zwarthoff, E. C., Riegman, P. H., Deelen, W. H., van den Ouweland, A. M. W. et al. (1995). Positional mapping of loci in the DiGeorge critical region at chromosome 22q11 using a new marker (D22S183). *Hum. Genet.* **96**, 133-141.

Nan, X., Meehan, R. R. and Bird, A. (1993). Dissection of the methyl-CpG binding domain from the chromosomal protein MeCP2. *Nucl. Acids Res.* **21**, 4886-4892.

Nan, X., Tate, P., Li, E. and Bird, A. (1996). DNA methylation specifies chromosomal localization of MeCP2. *Mol. Cell Biol.* **16**, 414-421.

Nan, X., Campoy, F. J. and Bird, A. (1997). MeCP2 is a transcriptional repressor with abundant binding sites in genomic chromatin. *Cell* **88**, 471-481.

Nan, X., Ng, H. H., Johnson, C. A., Laherty, C. D., Turner, B. M., Eisenman, R. N. and Bird, A. (1998). Transcriptional repression by the methyl-CpG-binding protein MeCP2 involves a histone deacetylase complex. *Nature* **393**, 386-389.

Parseghian, M. H., Clark, R. F., Hauser, L. J., Dvorkin, N., Harris, D. A. and Hamkalo, B. A. (1993). Fractionation of human H1 subtypes and characterization of a subtype-specific antibody exhibiting non-uniform nuclear staining. *Chromosome Res.* **1**, 127-139.

Payen, E., Verkerk, T., Michalovich, D., Dreyer, S. D., Winterpacht, A., Lee, B., De Zeeuw, C. I., Grosveld, F. and Galjart, N. (1998). The centromeric/nucleolar protein ZFP-37 may function to specify neuronal nuclear domains. *J. Biol. Chem.* **273**, 9099-9109.

Peters, A., Palay, S. L. and Webster, H. d. (1991). *The Fine Structure of the Nervous System*. New York/Oxford: Oxford University Press.

Reynaud, C., Bruno, C., Boullanger, P., Grange, J., Barbesti, S. and Niveleau, A. (1992). Monitoring of urinary excretion of modified nucleosides in cancer patients using a set of six monoclonal antibodies. *Cancer Lett.* **61**, 255-262.

Rivera-Leon, R. and Gerbi, S. A. (1997). Delocalization of some small nucleolar RNPs after actinomycin D treatment to deplete early pre-rRNAs. *Chromosoma* **105**, 506-514.

Sambrook, J., Fritsch, E. F. and Maniatis, T. (1989). *Molecular Cloning: a Laboratory Manual*. New York: Cold Spring Harbor Laboratory Press.

Santama, N., Dotti, C. G. and Lamond, A. I. (1996). Neuronal differentiation in the rat hippocampus involves a stage-specific reorganization of subnuclear structure both in vivo and in vitro. *Eur. J. Neurosci.* **8**, 892-905.

Saurin, A. J., Shiels, C., Williamson, J., Satijn, D. P., Otte, A. P., Sheer, D. and Freemont, P. S. (1998). The human polycomb group complex associates with pericentromeric heterochromatin to form a novel nuclear domain. *J. Cell Biol.* **142**, 887-898.

Sewalt, R. G., van der Vlag, J., Gunster, M. J., Hamer, K. M., den Blaauwen, J. L., Satijn, D. P., Hendrix, T., van Driel, R. and Otte, A. P. (1998). Characterization of interactions between the mammalian polycomb-group proteins Enx1/EZH2 and EED suggests the existence of different mammalian polycomb-group protein complexes. *Mol. Cell Biol.* **18**, 3586-3595.

Shi, Y. P., Mohapatra, G., Miller, J., Hanahan, D., Lander, E., Gold, P., Pinkel, D. and Gray, J. (1997). FISH probes for mouse chromosome identification. *Genomics* **45**, 42-47.

Sinclair, D. A. and Guarente, L. (1997). Extrachromosomal rDNA circles – a cause of aging in yeast. *Cell* **91**, 1033-1042.

Smith, J. S. and Boeke, J. D. (1997). An unusual form of transcriptional silencing in yeast ribosomal DNA. *Genes Dev.* **11**, 241-254.

Stein, G. S., van Wijnen, A. J., Stein, J. L., Lian, J. B., McNeil, S. and Pockwinse, S. M. (1999). Transcriptional control within the three-dimensional context of nuclear architecture: requirements for boundaries and direction. *J. Cell. Biochem.* (suppl.) 24-31.

van der Vlag, J. and Otte, A. P. (1999). Transcriptional repression mediated by the human polycomb-group protein EED involves histone deacetylation. *Nature Genet.* **23**, 474-478.

van Lohuizen, M., Tijms, M., Voncken, J. W., Schumacher, A., Magnuson, T. and Wientjens, E. (1998). Interaction of mouse polycomb-group (Pc-G) proteins Enx1 and Enx2 with Eed: indication for separate Pc-G complexes. *Mol. Cell Biol.* **18**, 3572-3579.

Wijgerde, M., Grosveld, F. and Fraser, P. (1995). Transcription complex stability and chromatin dynamics in vivo. *Nature* **377**, 209-213.

Zlatanova, J. and Yaneva, J. (1991). Histone H1-DNA interactions and their relation to chromatin structure and function. *DNA Cell Biol.* **10**, 239-248.